Molecular Biology of the Cell
Vol. 16, 433–445, February 2005

β1-Integrin Orients Epithelial Polarity via Rac1 and Laminin[D]

Wei Yu,* Anirban Datta,* Pascale Leroy,* Lucy Erin O'Brien,* Grace Mak,† Tzuu-Shuh Jou,‡ Karl S. Matlin,† Keith E. Mostov,* and Mirjam M.P. Zegers*§‖

*Departments of Anatomy and Biochemistry and Biophysics, School of Medicine, University of California San Francisco, San Francisco, CA 94143; ‡Department of Internal Medicine, National Taiwan University Hospital and National Taiwan University College of Medicine, Taipei, 100 Taiwan; and †Epithelial Pathobiology, Department of Surgery, University of Cincinnati College of Medicine, Cincinnati, OH 45267-0581

Submitted May 27, 2004; Revised November 1, 2004; Accepted November 19, 2004
Monitoring Editor: Jean Schwarzbauer

Epithelial cells polarize and orient polarity in response to cell–cell and cell–matrix adhesion. Although there has been much recent progress in understanding the general polarizing machinery of epithelia, it is largely unclear how this machinery is controlled by the extracellular environment. To explore the signals from cell–matrix interactions that control orientation of cell polarity, we have used three-dimensional culture systems in which Madin-Darby canine kidney (MDCK) cells form polarized, lumen-containing structures. We show that interaction of collagen I with apical β1-integrins after collagen overlay of a polarized MDCK monolayer induces activation of Rac1, which is required for collagen overlay-induced tubulocyst formation. Cysts, comprised of a monolayer enclosing a central lumen, form after embedding single cells in collagen. In those cultures, addition of a β1-integrin function-blocking antibody to the collagen matrix gives rise to cysts that have defects in the organization of laminin into the basement membrane and have inverted polarity. Normal polarity is restored by either expression of activated Rac1, or the inclusion of excess laminin-1 (LN-1). Together, our results suggest a signaling pathway in which the activation of β1-integrins orients the apical pole of polarized cysts via a mechanism that requires Rac1 activation and laminin organization into the basement membrane.

INTRODUCTION

Polarization of cells is a fundamental process in biology. Epithelial cells polarize into apical and basolateral poles. Much has been learned recently about the mechanisms of epithelial polarization. Three major polarization complexes, the Par3/Par6/atypical protein kinase C (aPKC), Crumbs/PATJ/Stardust, and Scribble/Discs Large/Lethal Giant Larvae complexes are conserved from *Caenorhabditis elegans* and *Drosophila* to mammals and are essential for epithelial polarization (Roh and Margolis, 2003; Macara, 2004). Cell polarization also requires interactions of the cells with each other and the extracellular matrix (ECM), as well as polarized organization of the cytoskeleton and membrane traffic, although how these processes are connected to the three polarization complexes is largely obscure (Vega-Salas *et al*., 1987; Yeaman *et al*., 1999; O'Brien *et al*., 2002; Mostov *et al*., 2003; Nelson, 2003; Zegers *et al*., 2003).

Formation of epithelial tissues requires that the orientation of polarity of individual epithelial cells be coordinated in space and time. This was underappreciated in studies using cells grown on filter supports, because the filter provides an overriding extrinsic cue to orient the cells with the basolateral surface facing the filter and the apical surface opposite. Building on earlier observations (Wang *et al*., 1990a), we found that generation of epithelial polarity can be uncoupled from the orientation of that polarity (O'Brien *et al*., 2001). Madin-Darby canine kidney (MDCK) epithelial cells grown in three-dimensional (3D) collagen gels form cysts, where the apical surface of a polarized monolayer of cells faces a central lumen. Importantly, expression of a dominant negative mutant of the Rho-family GTPase, Rac1 (N17Rac1), causes inversion of polarity, so that the apical surface is at the periphery of the lumen-less cysts. This suggests that Rac1 is a component of a polarity orientation pathway. More generally, Rho-GTPases control various processes that regulate cell polarity, including cytoskeletal dynamics, polarized protein trafficking, and cell adhesion (Hall, 1998; Etienne-Manneville and Hall, 2002; Van Aelst and Symons, 2002).

Orientation of polarity also requires interaction of the epithelial cell with the ECM. Such interactions often involve integrins, heterodimers of α and β subunits. Integrin-mediated adhesion provides signals that control cell motility, proliferation, survival, differentiation, and gene expression (Giancotti and Ruoslahti, 1999). The role of β1-containing integrins in orientation of polarity has been studied in MDCK cells in some detail. In suspension culture (i.e., without exogenous ECM), these cells form hollow cysts where a monolayer of cells has the apical surface facing the outside (i.e., opposite to that of the collagen-grown cysts described above) (Wang *et al*., 1990b). When these cysts are placed in a collagen I gel, polarity reverses by a mechanism

Article published online ahead of print in *MBC in Press* on December 1, 2004 (http://www.molbiolcell.org/cgi/doi/10.1091/mbc.E04-05-0435).

[D] The online version of this article contains supplemental material at *MBC Online* (http://www.molbiolcell.org).

§ Present address: Epithelial Pathobiology, Department of Surgery, The Vontz Center, University of Cincinnati College of Medicine, 3125 Eden Avenue, ML0581, Cincinnati, OH 45267-0581.

‖ Corresponding author. E-mail address: zegersm@ucmail.uc.edu.

that depends on β1 integrin (Ojakian and Schwimmer, 1994). In a similar process, a β1 integrin-dependent reorientation of the apical pole is induced after overlaying the apical surface of a filter-grown, polarized monolayer with collagen I (Schwimmer and Ojakian, 1995; Zuk and Matlin, 1996; Ojakian *et al.*, 2001). Laminins are a family of heterotrimeric proteins consisting of α, β, and γ chains. Currently, 15 different laminin isoforms (LN-1–LN-15) have been identified (Miner and Yurchenco, 2004). Although it has been known for a long time that MDCK cells secrete laminin from their basolateral surface (Caplan *et al.*, 1987), the particular isoforms still have to be identified. Normally, laminin secreted by MDCK cell cysts grown in collagen I gels assembles into a basement membrane (BM)-like network surrounding the cyst (O'Brien *et al.*, 2001). In cysts of MDCK cells expressing N17Rac1, laminin is not properly assembled into this BM. However, addition of a high concentration of exogenous LN-1, which can spontaneously assemble, can largely rescue the inverted polarity of N17Rac1 cysts, yielding nearly normal cysts with the apical surfaces of the cells facing a central lumen.

Here, we show that β1 integrin lies upstream of Rac1 in a pathway controlling orientation of polarity. Collagen I binding to β1 integrin causes activation of Rac1. This in turn orients the polarity of the cell, in a process that also requires laminin-dependent assembly of BM.

MATERIALS AND METHODS

Antibodies and Reagents

Ascites of function-blocking rat monoclonal antibody AIIB2 anti-β1-integrin were a gift from Caroline Damsky (Department of Stomatology, School of Dentistry, University of California, San Francisco, CA). Concentrations of this rat IgG in the mouse ascites were determined by Western blotting, by using purified rat IgG as a standard. Functionality of the AIIB2 antibodies in the ascites was confirmed by analyzing adhesion to collagen I and LN-1, by using affinity-purified AIIB2 as a standard. AIIB2 was affinity purified using a HiTrap protein G column (Amersham Biosciences, Piscataway, NJ). Both analyses indicated a similar concentration of AIIB2 in the ascites. Other primary antibodies used in this study were: mouse anti-gp135 (from George Ojakian, Department of Anatomy and Cell Biology, SUNY-Downstate Medical Center), rabbit anti-β-catenin, mouse anti-Rac1 (Santa Cruz Biotechnology, Santa Cruz, CA), mouse anti-*cis*-Golgi enzyme GM130 (BD Transduction Laboratories, Lexington, KY), rabbit anti-occludin (Zymed Laboratories, South San Francisco, CA), rat IgG (Pierce Chemical, Rockford, IL), rat GoH3 anti-α6 integrin, rabbit anti-α3 integrin, mouse anti-collagen IV (Chemicon International, Temecula, CA), and mouse anti-myc and mouse anti-β-tubulin (Sigma-Aldrich, St. Louis, MO). Rabbit anti-LN-1 antiserum (Sigma-Aldrich) was raised against LN-1, which consists of α1, β1, and γ1 chains. Secondary antibodies used were highly cross-absorbed anti-mouse Alexa Fluor 555 and anti-rabbit Alexa Fluor 488 (Molecular Probes, Eugene, OR). Actin filaments were stained with Alexa Fluor 488 or 549 phalloidin (Molecular Probes). Nuclei were labeled with DRAQ5 (Biostatus, Leicester, United Kingdom). L-[^{35}S]Methionine protein labeling mix was from PerkinElmer Life and Analytical Sciences (Boston, MA).

Cell Culture

MDCK cells were maintained in minimal essential medium (MEM) containing Earle's balanced salt solution (Cellgro, Washington, DC) supplemented with 5% fetal bovine serum and antibiotics in 5% CO_2, 95% air. T23 MDCK cells expressing N17Rac1 and V12Rac1 under control of the tetracycline-repressible transactivator (Jou and Nelson, 1998) were maintained in growth medium with 20 ng/ml doxycycline.

For collagen gel overlays, confluent cells grown on 24-mm Transwell (0.4-μm pore size) were covered with type I collagen gel (66% vitrogen, 3 mg/ml, Cohesion; Palo Alto, CA) in growth medium, essentially as described previously (Zuk and Matlin, 1996), and cultured in MEM for 5 d.

Cyst cultures were prepared as described previously (O'Brien *et al.*, 2001; Yu *et al.*, 2003). Briefly, cells were trypsinized into a single-cell suspension of 4×10^4 cells/ml in type I collagen gel. Then, 160 μl of cells in collagen solution were plated onto Nunc filters (10 mm in diameter, 0.02-μm pore) for immunostaining, and 300 μl was plated on the top of a cell-free gelled collagen layer for biochemical experiments. The collagen mixture was allowed to gel at 37°C and then medium was added. Cells were fed every 3 d and grown for 7–10 d until cysts with lumen were formed. To treat cysts with AIIB2, the antibody was added to the collagen gel as well as to the culture medium in a final concentration of 8 μg/ml. For the laminin rescue experiment, LN-1 (BD Biosciences, San Jose, CA) was added to the collagen I solution at a final concentration 500 μg/ml (final collagen I concentration was 1.0 g/ml). For the collagen IV rescue experiment, collagen IV (BD Biosciences) was added to collagen I solution at a final concentration of 0.15 mg/ml (final concentration of collagen I was 1.33 g/ml). To induce the V12Rac1 expression in cyst cultures, cells expressing V12Rac1 were stimulated with 2.5 mM sodium butyrate overnight in the absence of doxycycline. Cells were plated in collagen 6 h after removing sodium butyrate and grown in the absence of both doxycycline and sodium butyrate.

Immunofluorescence Staining

The procedure for the immunofluorescence staining of cysts cultured in collagen gel was previously described in detail (Pollack *et al.*, 1998; O'Brien *et al.*, 2001; Yu *et al.*, 2003). Samples were rinsed with phosphate-buffered saline (PBS)+ (PBS containing Mg^{2+} and Ca^{2+}) twice quickly, treated with collagenase type VII (Sigma-Aldrich) at 37°C for 10 min, and fixed with 3% paraformaldehyde for 30 min. Cells were permeabilized with 0.25% Triton X-100 in PBS for 10 min, quenched with 50 mM NH_4Cl for 10 min, and blocked with 0.7% gelatin in PBS/0.1% saponin for 30 min. Samples were then incubated in primary antibodies at 4°C overnight, followed by an overnight incubation at 4°C with Alexa Fluor 532- or Alexa Fluor 488-conjugated secondary antibody (1:200) dilution and Alexa Fluor 488 phalloidin (1:50). Samples were mounted with Prolong antifade (Molecular Probes). To stain laminin and collagen IV staining, cysts were incubated with anti-LN-1 (1:100) or anti-collagen IV (1:100) for 4 h before fixation.

Cells overlaid with collagen gel were rinsed with PBS+. Then, the collagen gel was gently removed, and the cells on the filter were fixed with 3% paraformaldehyde for 20 min, quenched with 50 mM NH_4Cl for 10 min, and blocked and permeabilized with 0.7% gelatin in PBS/0.1% saponin for 30 min. Samples were incubated with primary antibodies overnight at 4°C, followed by incubation with Alexa Fluor 532 and Alexa Fluor 488-conjugated secondary antibodies (1:200) at 37°C for 1 h. After washing, the samples were incubated with DRAQ5 at a 1:1000 dilution for 5 min at 37°C, and mounted with Fluorosave (Calbiochem, San Diego, CA).

Transmission Electron Microscopy

Cysts grown in collagen gel in the absence or presence of AIIB2 were fixed with 2% glutaraldehyde and 0.8% paraformaldehyde. The procedures for electron microscopy were described in detail previously (O'Brien *et al.*, 2001). Ultrathin sections were examined with a transmission electron microscope (Zeiss 10CA).

Image Analysis

To quantitate cyst polarity, cysts were stained for gp135, β-catenin, and nuclei and analyzed with a Zeiss 510 LSM confocal microscope. Cysts with gp135 staining at the interior surface, and β-catenin facing the surrounding ECM were identified as cysts with normal polarity (interior apical pole). Cysts that had gp135 at the peripheral surface and in which β-catenin was absent from the periphery were considered as cysts with inverted polarity (peripheral apical pole). Per condition, 300 cysts were analyzed.

Immunoprecipitaton and Western Blotting

Laminin and integrin levels in cysts were determined by immunoprecipitation or Western blot as described in detail previously (O'Brien *et al.*, 2001) with some modifications. To determine β1 and α3 integrin levels and cell-associated laminin, cysts were isolated from collagen by collagenase treatment. To detect intracellular laminin levels, isolated cysts were treated with trypsin (O'Brien *et al.*, 2001). Lysates of isolated cysts were normalized for protein concentration using a BCA assay (Pierce Chemical). Laminin in the culture medium and in the solubilized collagen gel was determined by immunoprecipitation. The concentration of SDS in the samples was adjusted to 0.5%, and samples were normalized based on the protein concentration of isolated cysts. Western blotting of β-tubulin was used as control for normalization of lysates used for the immunoprecipitation of the solubilized cyst and for lysates of the isolated cysts.

Metabolic Labeling of Cysts

Cysts, grown in the absence or presence of AIIB2 were metabolically labeled for 20 h with 100 μCi of L-[^{35}S]Met in Met/Cys-free DMEM, containing 10% normal growth medium and 10% fetal calf serum. The cysts in collagen were washed with PBS, and cyst-associated and intracellular laminin was immunoprecipitated as described above, by using anti-LN1 antiserum. Immunoprecipitated proteins were separated on a 6% SDS-PAGE gel and radiolabeled proteins were identified by autoradiography as described previously (Schoenenberger *et al.*, 1994)

Rac1 Activation Assay

Confluent MDCK cells grown on filter were overlaid with collagen solution for the indicated time periods. Both filter and collagen gel, which had a total volume of 450–500 μl, were transferred to a tube containing 500 μl of ice-cold 2× Gold lysis buffer (2% Triton X-100, 40 mM Tris-HCl, pH 7.5, 1000 mM NaCl, 20 mM $MgCl_2$, 30% glycerol, 1 mM dithiothreitol, and EDTA-free protease inhibitors; Roche Diagnostics, Indianapolis, IN), To determine GTP-Rac1 levels in V12Rac1-expressing cells, collagen and overlay cultures were harvested and diluted in equal volumes of 2× GLB after 7-d culture. Samples were then tumbled at 4°C for 20 min. This treatment dissolved >95% of the collagen gel. Samples were then centrifuged in a microcentrifuge at 15,000 rpm for 5 min to remove the remaining fragments of collagen and cell debris. A 50-μl sample from the supernatant was taken aside for determination of Rac levels in the total lysate, and GTP loading on Rac1 was determined using a pull-down assay with GST-Pak3-CRIB beads as described previously (Hansen *et al*., 2001). Western blotting for β-tubulin levels in the total lysate served as loading control.

RNA Extraction and Reverse Transcription-Polymerase Chain Reaction (RT-PCR) Analysis of Laminin α Chains

RNA from cysts were extracted using the RNeasy Mini kit (QIAGEN, Valencia, CA). Cysts were homogenized in lysis buffer with a homogenizer and treated with 200 μg/ml protein kinase (QIAGEN) for 30 min previous to the RNA extraction on column. DNase I treatment was done directly on the column. 1 μg of total RNA was reverse transcribed, and relative RT-PCR was done as described previously (Leroy *et al*., 2004). The yield of cDNA was measured using the expression of the gene coding for glyceraldehyde-3-phosphate dehydrogenase (GAPDH) as an internal standard. Starting from 1 μl of cDNA, more than 20 cycles were necessary to detect GAPDH, and the volume of each cDNA was adjusted to give the same PCR signal strength for GAPDH after 23 cycles i.e., in its exponential amplification range. Laminin α5 chain exponential amplification range was tested and experiments were done with 38 cycles for laminin α5 and 23 cycles for GAPDH. Internal standard and the laminin α chain were amplified in the same tube (Meadus, 2003) with GAPDH primers added when 23 cycles remained for the amplification of laminin chain. Primers were as follows: for laminin α5 chain, forward: 5′ TGGGCAAGTATGTGGACCTC 3′ and reverse: 5′ TGCTGATGCAGCCACTGAAG 3′; and for GAPDH, forward: 5′ CAGTTGTGGATCTGACCTGC 3′ and reverse: 5′ CCTTGGAGGCCATGTAGACC 3′. Annealing was done at 55°C for laminin α5, and the expected fragments (500 base pairs for laminin α5 and 271 base pairs for GAPDH) were visualized on a 2% agarose gel.

RESULTS

Activation of β1-Integrin by Collagen Overlay Induces Rac1 Activation

Application of collagen I gel overlay to the apical domain of a polarized monolayer of MDCK cells induces dramatic changes in the organization of the cells and the orientation of their polarity. Specifically, the apical domain is reoriented away from the new ECM-cell contact site, and multilayered, polarized lumen-containing structures, or tubulocysts are formed (Schwimmer and Ojakian, 1995; Zuk and Matlin, 1996; compare control monolayers in Figure 1A and collagen overlays in C). This therefore provides a simple system to study how collagen I is involved in the orientation and organization of epithelial cells and can be considered intermediate in complexity and physiological relevance between growing cells as a monolayer on a filter and growth as cysts in thick collagen gels. Although not affecting the monolayer in the absence of overlay (Figure 1B), the β1 integrin function-blocking antibody AIIB2, but not nonspecific control antibodies (Figure 1, E and F), inhibited the collagen I-induced formation of tubulocysts when added to the collagen I (Figure 1D, (Schwimmer and Ojakian, 1995; Zuk and Matlin, 1996).

Rac1 regulates orientation of apical polarity in MDCK cysts grown in collagen (O'Brien *et al*., 2001) and is activated through integrins in 3D cultures of mammary epithelial cells (Zahir *et al*., 2003). To determine whether Rac1 has a role in the pathway downstream of β1 integrin that regulates tubulocyst formation, we examined whether collagen I overlay activates Rac1. We analyzed Rac1-GTP levels by using a Cdc42/Rac interactive binding (CRIB)-domain pull-down assay (Price *et al*., 1998). For this experiment, the collagen overlay approach is advantageous compared with growing cysts in thick collagen gels, in that the overlay technique causes synchronous interaction of collagen I with large numbers of polarized cells, induces synchronous remodeling of

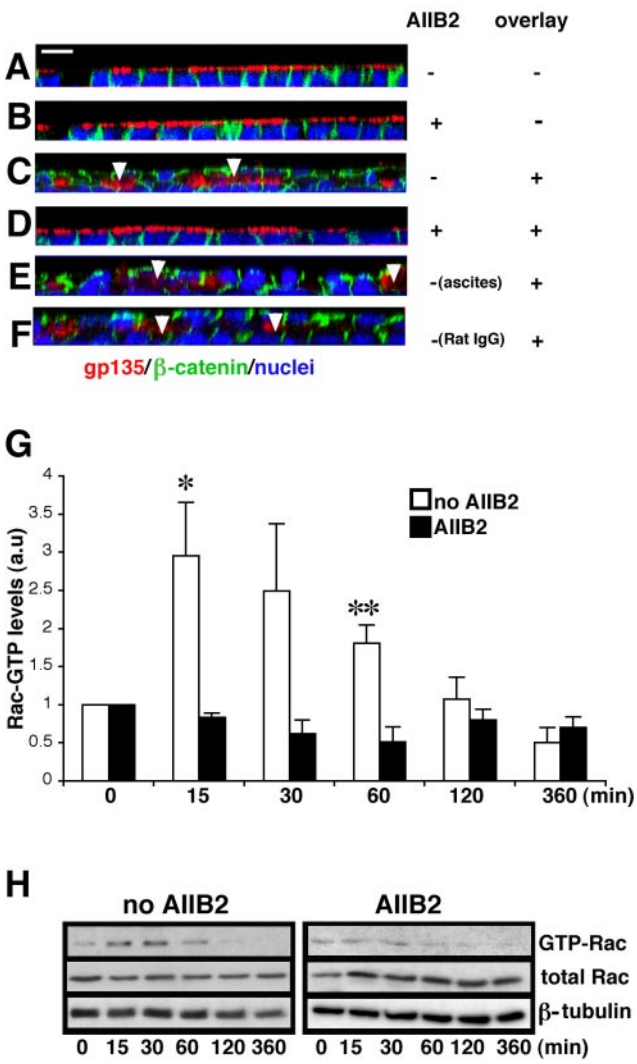

Figure 1. β1 integrin-mediated activation of Rac1 is required for the formation of tubulocysts upon collagen overlay. (A–F) Confocal images of gp135 (red) and β-catenin (green) of vertical sections show MDCK cells grown on Transwell filters at indicated conditions. (A) Confluent MDCK in the absence of AIIB2 and collagen gel have a polarized monolayer morphology. (B) Treatment with 8 μg/ml AIIB2 for 5 d does not change the monolayer phenotype. (C) MDCK cells overlaid on the apical surface with type I collagen gel for 5 d induces the formation of tubulocysts. (D) Addition of AIIB2 to the collagen inhibits tubulocyst formation in response to apical collagen overlay. (E and F) Control Rat IgG and mouse ascites 9E10 do not inhibit tubulocyst formation in response to collagen overlay. Arrowheads indicate lumens. (G) Time course of Rac1 activation by collagen overlay in the absence (white column) or presence (black column) of AIIB2 was assessed by a GST-CRIB-PAK pull-down assay. The apical surface of a polarized MDCK monolayer was overlaid with collagen for the indicated periods. Results were normalized to GTP-Rac1 levels in the 0-min lane. The graph represents five independent experiments ± SD. *$p < 0.03$, **$p < 0.01$, relative to no overlay (0 min). (H) Representative Western blots of Rac1 activation for Figure 1G, β-tubulin serves as loading control. Bar, 10 μm.

cell polarity, and permits the rapid isolation of the cells for measurement of the level of Rac1-GTP. Collagen overlay resulted in a threefold increase in GTP-Rac1 levels after 15 min, which was the earliest time point we were able to analyze after overlay (Figure 1, G and H). The activation of Rac1 was transient and 6 h after overlay, GTP-Rac1 levels had declined to control levels. In contrast, when cells were overlaid in the presence of the AIIB2 antibody, Rac1 activation was not observed. Rather, we found that 30 and 60 min after overlay, AIIB2 treatment resulted in GTP-Rac1 levels that were statistically indistinguishable from (and slightly below) baseline. Hence, these results suggest that apical collagen overlay activates Rac1 via activation of β1 integrins.

Rac1 Activation Is Required for Tubulocyst Formation

We next examined whether the increase in GTP-Rac1 was required for tubulocyst formation. We used MDCK cells that expressed dominant-negative (N17Rac1) or activated (V12Rac1) forms of Rac1 under control of a tetracycline-repressible promoter system (Jou and Nelson, 1998). In this system, ectopic gene expression is repressed by addition of 20 ng/ml doxycycline (Dox) to the culture medium. Control experiments showed that, when not induced (+Dox), collagen I overlay resulted in elevated GTP-Rac1 level after 15 min, similar to untransfected controls (compare Figure 2A, +Dox, to Figure 1H). As expected, no GTP-Rac1 was observed in N17Rac1-expressing cells, either with or without collagen overlay, whereas GTP-Rac1 levels in V12Rac1-expressing cells were consistently high but not affected by collagen overlay (Figure 2A, −Dox).

In the absence of overlay, the monolayer was not affected by expression of N17Rac1 (Figure 2B, compare the nonexpressing cells in 2B-1 with the N17Rac1-expressing cells in 2B-2). However, unlike the noninduced N17Rac1 control cells (2B-3), which formed well-established tubulocysts, cells expressing N17Rac1 did not form tubulocysts upon collagen overlay (2B-4). Instead, they retained their polarized phenotype and resembled monolayers that were overlaid in the presence of AIIB2 (compare Figure 2B-4 with Figure 1D). Cells that expressed the activated V12Rac1 mutant (2B-6), but not the noninduced controls (2B-5) formed slightly irregular and partly flattened monolayers in the absence of overlay, but they did not develop tubulocysts on their own. On collagen I overlay, the V12Rac1-expressing cells formed tubulocysts similar to noninduced cells (compare 2B-8 with 2B-7), although they formed generally faster compared with noninduced cells (our unpublished data). Moreover, in contrast to noninduced cells (2B-9), V12Rac1 expression rescued the AIIB2-induced block on tubulocysts formation (2B-10). Together, these data indicate that the Rac1 activation we observed upon collagen overlay is downstream of activated β1 integrin and necessary for tubulocyst formation. However, because V12Rac1 did not induce formation of tubulocysts in the absence of collagen overlay (2B-6), Rac1 activation is not sufficient for this morphological response in monolayer cultures. This may suggest that other signals activated by β1 integrins are required for tubulocyst formation as well. Alternatively, collagen may act as a mechanical support needed for attachment and cellular movements and/or for deposition of autocrine signaling molecules such as laminin.

β1 Integrins Regulate Orientation of Polarity in MDCK Cysts via Rac1

Single MDCK cells embedded in a collagen I matrix form cysts with an apical pole oriented toward the central lumen and a basolateral pole toward the matrix. Expression of

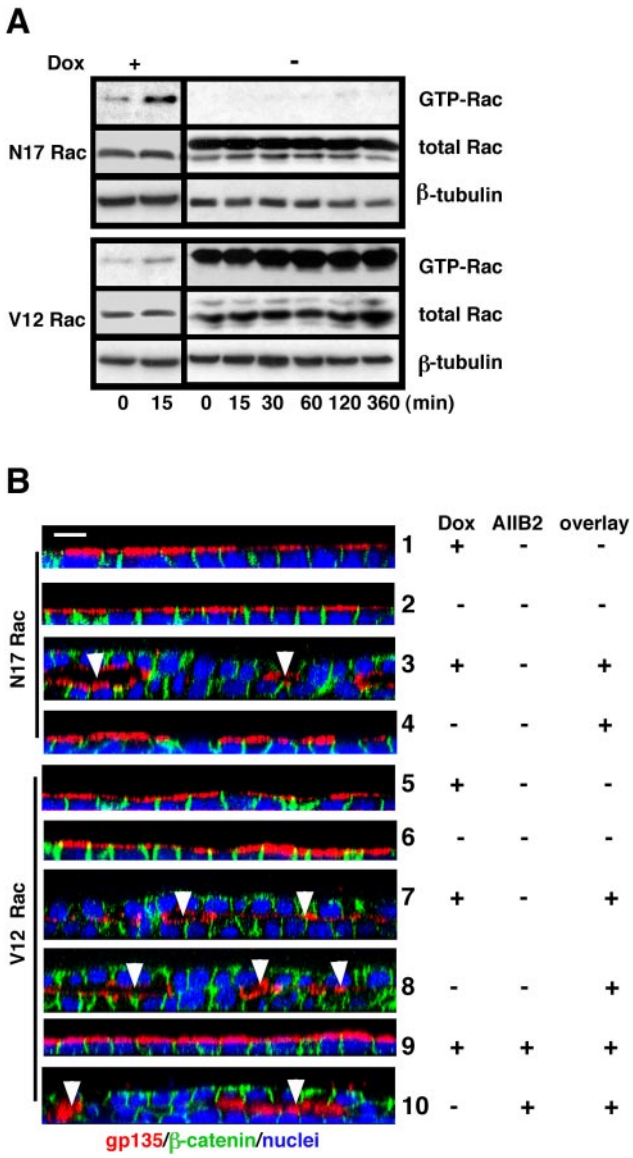

Figure 2. Rac1 activation is required for tubulocyst formation. (A) Endogenous and mutant Rac1 protein levels and Rac1 activation in cells that express myc-tagged N17Rac1 and V12Rac1 under control of the tetracycline-repressible transactivator. MDCK monolayers grown on filters in the absence or presence of Dox were overlaid with collagen gel for the indicated times. Western blots show total Rac1 expression. Double bands in total lysates of mutant Rac1-expressing cells (−Dox) show expression of endogenous (top band) and myc-tagged mutant Rac1 (bottom band). Activated Rac1 (GTP-Rac1) was determined by a GST-CRIB-PAK pull-down assay. GTP-Rac1 was not detected in cells expressing N17Rac1, but it was high in V12Rac1 cells. β-Tubulin was used as a loading control. (B) Vertical sections of monolayers stained for gp135 (red) and β-catenin (green) show mutant Rac1-expressing cells grown with or without collagen overlay and AIIB2 as indicated. Both noninduced and induced N17Rac1 cells remain a polarized monolayer in the absence of collagen overlay (2B-1 and 2B-2). Noninduced N17Rac1 cells develop normal tubulocysts (2B-3), whereas N17Rac1-expressing cells do not form tubulocysts (2B-4). Both noninduced V12Rac1 and induced V12Rac1 cells have polarized monolayer phenotypes in the absence of collagen overlay (2B-5 and 2B-6) and form tubulocysts in the presence of collagen overlay (2B-7 and 2B-8). When AIIB2 is present in the collagen overlay, tubulocyst formation is blocked in noninduced V12Rac1 cells (2B-9), but not in cells expressing V12Rac1 (2B-10). Arrowheads indicate lumens. Bar, 10 μm.

N17Rac1 causes an inversion of apical polarity in these cysts (O'Brien *et al*., 2001). Because the data indicate that apical pole reorientation during tubulocyst formation requires signaling from β1 integrin to Rac1, we asked whether the same pathway controls the de novo formation of the apical pole in MDCK cysts. To this end, we grew cysts in the presence of 8 μg/ml AIIB2 antibody for 7–10 d. The phenotype of cysts grown in presence of AIIB2 (Figure 3 B, B′, D, F, F′, and H) was strikingly similar to what we observed previously in cysts expressing N17Rac1 (O'Brien *et al*., 2001). Analysis by immunofluorescence staining revealed that markers for an apical membrane protein (gp135), a tight junctional marker (occludin), and a Golgi marker (GM130) that are normally oriented toward the cyst lumen were oriented toward the collagen matrix upon AIIB2 treatment (compare Figure 3A, C, E, and E′ with 3B, D, F, and F′). Electron microscopic images were consistent with these results and showed that structures resembling intercellular junctional complexes were near the lumen in control cells (Figure 3G, arrowhead), whereas they were localized at cell-cell contacts facing the collagen in AIIB2-treated cysts (Figure 3H, arrowhead). Costaining of cysts with apical gp135 and basolateral β-catenin showed that the polarity of cells within AIIB2-treated cyst was inverted, rather than randomized; in both control (Figure 3, A and A′) and AIIB2-treated cysts (Figure 3, B and B′), the localization of apical and basolateral antigens excluded each other. The latter finding was in contrast to cells expressing N17Rac1, which have inverted apical polarity, but basolateral markers, including β-catenin (our unpublished data) were found at all cell surfaces (O'Brien *et al*., 2001). A possible explanation is that in addition to activating Rac1, binding of β1 integrins to collagen also may activate other signaling components that regulate epithelial morphogenesis. Finally, AIIB2 cysts had filled lumens, suggesting alterations in cell proliferation and/or apoptosis (our unpublished data); this will be the subject of future investigation.

The cyst phenotype induced by AIIB2 treatment was specific for inhibition of β1 integrins. Control experiments showed that neither rat IgG1 (Figure 3I) in a concentration range of 6–60 μg/ml nor nonreactive antibodies added as an ascites (our unpublished data) affected the morphology of the cysts. Moreover, the concentrations of AIIB2 required to inhibit adhesion to collagen I strongly correlated with the ability to induce a phenotype in cysts. Specifically, addition of 8 μg/ml AIIB2 resulted in a 95% inhibition of adhesion to collagen I (our unpublished data) in a standard adhesion assay (Schoenenberger *et al*., 1994) and gave rise to cyst cultures in which >90% of cysts had an inverted phenotype (Figure 5D). Much higher concentrations of AIIB2, up to 80 μg/ml, yielded similar results. Addition of 1 μg/ml AIIB2, on the other hand, resulted in a 35% inhibition of adhesion and induced a phenotype in ~50% of the cysts (our unpublished data).

MDCK cells express α2β1, α3β1, and α6β4 integrin heterodimers (Schoenenberger *et al*., 1994). The β1-containing integrins, but not α6β4, act as receptors for collagen I, IV, and LN-1 (Schoenenberger *et al*., 1994). Because the α6 integrin function-blocking antibody GoH3 inhibits adhesion to ECM secreted by MDCK cells (our unpublished data), α6β4 is likely to interact with another, currently unidentified component of the endogenous ECM of MDCK. We found that inhibition of the α6β4 integrin with GoH3 did not affect the phenotype of the cysts (Figure 3J), consistent with our findings that the AIIB2-induced phenotype specifically depends on inhibition of β1-containing integrins.

We next attempted to identify which β1-containing integrin was responsible for the AIIB2-induced phenotype. None of the known function-inhibiting anti-α2 and anti-α3 integrin antibodies that were available to us inhibited adhesion of MDCK cells to collagen I (our unpublished data). Hence, we were unable to test the effect of inhibition of these α integrin subunits on cyst cultures. Western blot analysis of AIIB2-treated cysts however, showed that β1 integrin levels were unchanged but that levels of α3-integrin were decreased by 80% compared with untreated controls (Figure 3K). Because β1 integrin levels are found in excess in MDCK cells (Schoenenberger *et al*., 1994), these data suggest a possible role for α3β1 integrin in normal cyst morphogenesis.

Inhibition of β1 Integrins Affects Laminin Organization

Cells in MDCK cysts secrete and assemble laminin into a BM-like network around the cyst periphery. The BM-like network produced by MDCK may not be as fully developed as basement membranes seen underlying most epithelia in vivo, but as described below it contains laminin and collagen IV organized into a network(s), and for the purposes of this article, we refer to it simply as a BM. We recently reported that N17Rac1-expressing cysts do not assemble laminin into this BM correctly. However, when cultured with an excess of LN-1, which spontaneously self-assembles through interaction of the β1 and γ1 chains (Yurchenco and Cheng, 1993) these cells formed lumen-containing cysts, with apical domains facing these lumens. These data indicated that Rac1 controls apical orientation via laminin (O'Brien *et al*., 2001).

As our data suggest that the AIIB2-induced phenotype is mediated by the inability of cells to activate Rac1 through β1 integrin, we examined whether the inversion of polarity in these cells was due to organization of laminin into BM as well. We analyzed laminin deposition by staining cysts with polyclonal antibodies raised against LN-1. LN-1 consists of the α1, β1, and γ1 chains. We found that the rabbit anti-laminin antiserum we used recognized the β1 and γ1 but not the α1 chain from MDCK cells (O'Brien *et al*., 2001). We stained cysts with laminin by adding the laminin antiserum to live cysts, followed by fixation and staining with a secondary antibody. This procedure only visualizes extracellular laminin. As shown in Figure 4A, laminin in untreated cysts occurred as a finely punctate pattern around the cell periphery at the cell–ECM interphase. In a projection of multiple confocal sections, laminin is seen to form a fine network surrounding the cyst (Figure 4A′). We take this as evidence that normal MDCK cysts organize laminin into a BM-like network around the cyst. In contrast, when cysts were grown in the presence of AIIB2, laminin staining around the cyst looked strikingly altered and very irregular (Figure 4B). We take this as an indication that the assembly or organization of the laminin into a BM-like network is very different from normal. The abnormal laminin organization is particularly evident in the projection images (Figure 4, A′ and B′), which were created by projecting serial confocal sections spanning the entire cyst (Supplementary Figure 1). Careful analysis of the individual confocal sections revealed that in AIIB2-treated cysts, some laminin seemed to be localized in the cyst interior, in between the individual cells. Because our staining procedure only stained laminin accessible from the outside of the cyst, it is still unclear why we detect this laminin, because tight junctions are located at the cyst periphery of these cysts. Preliminary data however, indicate that tight junctions in AIIB2-treated cysts have an abnormal structure (our unpublished data), which may explain why the laminin antiserum has access to the cyst

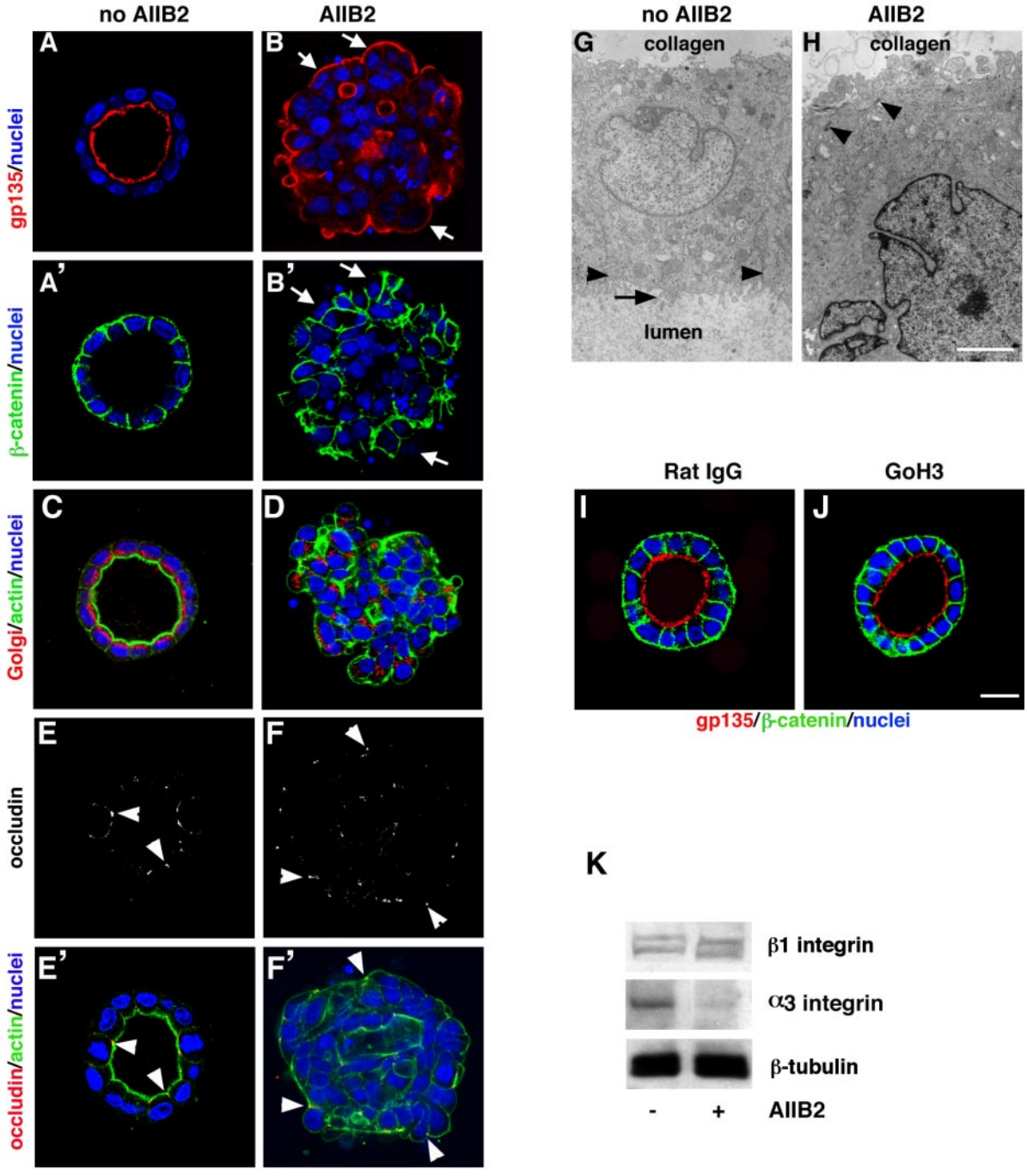

Figure 3. Inhibition of β1 integrins inverts apical polarity during cystogenesis and reduces expression of α3 integrin. (A–F) Cysts, grown in the absence (A, A′, C, E, and E′) or presence (B, B′, D, F, and F′) of 8 μg/ml AIIB2 were stained for markers of the apical pole (gp135, Golgi, and occludin) in red, for the basolateral membrane marker β-catenin (A′ and B′) or actin (C, D, E′, and F′) in green and for nuclei in blue. The tight junctional marker occludin is stained red in E′ and F′, and is shown alone for clarity in E and F. In untreated cysts, the apical marker gp135 (A), the Golgi marker GM130 (C), and occludin (E and E′) are localized at or toward the interior luminal surface, whereas staining of the basolateral membrane marker β-catenin (A′) is limited to cell–cell contacts and the peripheral surface and is excluded from the luminal surface (A and A′ represent the same cyst). Moreover, intense actin staining is observed around the lumen (C and E′). These staining patterns indicate a normal polarization. In contrast, polarity in AIIB2-treated cysts is inverted, as indicated by peripheral staining of gp135 (B), exclusion of β-catenin from peripheral surface (B′), orientation of the Golgi underneath the peripheral surface (D), and peripheral staining of occludin (F and F′). Arrows show that gp135 occurs at peripheral surface and β-catenin disappears from these areas in AIIB2-treated cysts (B and B′). Arrowheads point to junctional complexes, which are facing the lumen in control cysts (E and E′), and the periphery in AIIB2-treated cysts (F and F′). (G and H) Electron micrographs of cysts. In cysts grown in absence of AIIB2, tight junctions (arrowheads) at cell–cell contacts are close to the lumen and microvilli (arrow) face the lumen. In the presence of AIIB2, junctions face the collagen. (I) Addition of rat IgG as a control antibody does not affect cystogenesis. (J) Treatment with rat anti-integrin α6 antibody does not change the phenotype of cysts. (K) Western blot analysis shows that β1 integrin levels are not changed (bottom band of doublet represents a precursor form of β1 integrin), but α3 integrin is decreased in AIIB2-treated cysts. β-Tubulin levels are used as loading control. Bars, 10 μm (A–F, I, and J) and 2 μm (G and H).

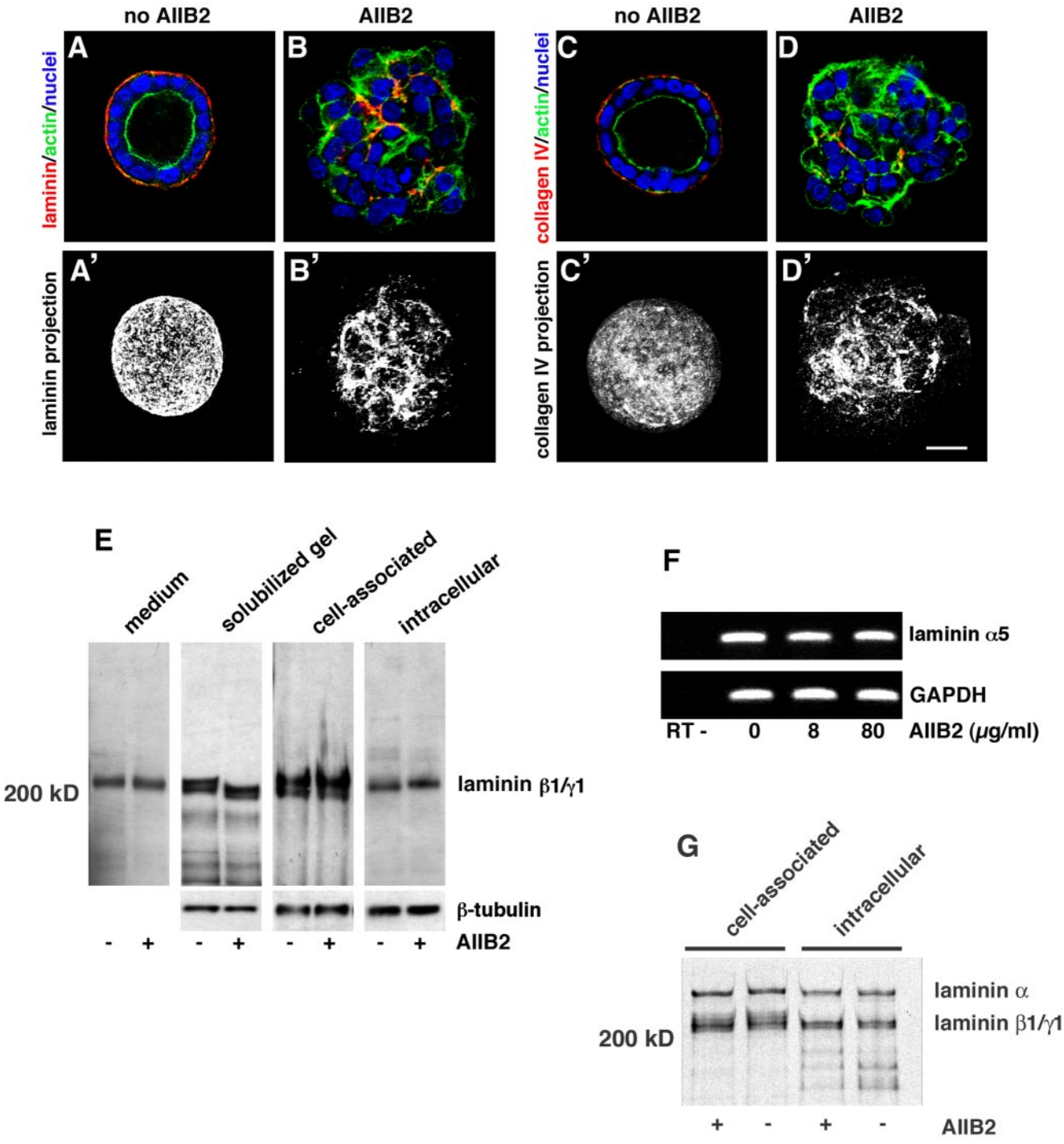

Figure 4. AIIB2-treated cysts have disorganized deposition of laminin and collagen IV. (A–H) Immunofluorescent staining of laminin (red in A and B), collagen IV (red in C and D), actin (green), and nuclei (blue) reveal the fine network of laminin and collagen IV on the peripheral surface of untreated cysts (A and C), but large aggregates in AIIB2-treated cysts (B and D). Projections of serial confocal sections more clearly demonstrate this difference between untreated (A′, laminin and C′, collagen IV) and AIIB2-treated cysts (B′, laminin and D′, collagen IV). (E) Western blotting of immunoprecipitated laminin shows no difference in secreted laminin (medium), total synthesized laminin (solubilized gel), cell-associated laminin (isolated cysts), and intracellular laminin (isolated and trypsin-treated cysts) between untreated and AIIB2-treated cysts. The $\beta1/\gamma1$ bands migrated at ~200 kDa. (F) RT-PCR analysis shows that treatment with AIIB2 does not significantly affect the expression levels of laminin $\alpha5$ chains. RT is control without reverse transcriptase. (G) Untreated or AIIB2-treated cysts were metabolically labeled with L-[^{35}S]methionine. Micrograph shows autoradiogram of laminin immunoprecipitated from isolated cysts, representing intracellular and cell-associated extracellular laminin, and from isolated cysts treated with trypsin to digest extracellular laminin (intracellular). In addition tot the $\beta1/\gamma1$ chains ~200 kDa, an ~400-kDa protein was immunoprecipitated, which likely respresents a coimmunoprecipitating laminin α chain from a $\beta1/\gamma1$-containing laminin heterotrimer. Note that AIIB2 does not affect levels of any laminin chain or ratio between the α and the $\beta1/\gamma1$ chains. Bar (A–D′), 10 μm.

interior. The staining pattern of collagen IV, another main component of the BM, was very similar to that of laminin. Thus, in untreated cysts we found collagen IV as a regular, BM-like network around the cyst periphery at the basal side of the cells (Figure 4, C and C′), whereas in AIIB2-treated cysts (Figure D and D′) it resembled the irregular staining we also observed for laminin. Together, these data suggest that inhibition of β1 integrin alters the organization of BM around MDCK cysts.

We analyzed whether the AIIB2-induced defect in BM deposition was due to changes in the synthesis or secretion of laminin. To this end, we determined levels of secreted and intracellular $\beta1/\gamma1$ laminin by immunoprecipitation and Western blotting (O'Brien *et al.*, 2001). Laminin levels were analyzed in the following pools: 1) the culture medium, which represents secreted laminin; 2) the collagen gel containing cysts in collagen, which together with pool 1 represents the total laminin synthesized; 3) cysts, isolated from the collagen gel after collagenase treatment, which represent cysts with associated BM and contains extracellular and intracellular cell-associated laminin; and 4) intracellular laminin, from isolated cysts treated with trypsin to digest the extracellular BM. As shown in Figure 4E, AIIB2 treatment did not affect $\beta1/\gamma1$ laminin levels in any of these pools.

Previous studies have shown that secretion of the LN-1 heterotrimer can be regulated by the α1-chain, which can be secreted independently from the $\beta1/\gamma1$ chains (Yurchenco *et al.*, 1997). Furthermore, β1 integrin-deficient mouse embryoid bodies do not secrete LN-1 because synthesis of the laminin α1 chain is shut off in these cells (Aumailley *et al.*, 2000). We therefore sought to investigate how AIIB2 affected synthesis and secretion of laminin α-chains. Because we were unable to detect any laminin α-chains by using Western blotting, we determined the effect of AIIB2 treatment on the laminin α-chain transcription by RT-PCR analysis. We detected robust expression of the laminin α3 (our unpublished data) and the α5 chains and found that both were unaffected by AIIB2 (Figure 4F; our unpublished data). However, we did not detect the laminin α1 chain (our unpublished data), indicating that LN-1 is apparently not expressed in MDCK. The laminin α3 chain is present in LN-5 ($\alpha3\beta2\gamma2$), LN-6 ($\alpha3\beta1\gamma1$), and LN-7 ($\alpha5\beta2\gamma1$). Although LN-5 is present in the kidney, it is unlikely that we detect this laminin form with the anti-LN-1 antiserum, because LN-1 does not share any of its chains with LN-5. In contrast, LN-10, which consists of the $\alpha5\beta1\gamma1$ chains, is the most abundant laminin expressed in the kidney and shares the β1 and γ1 laminin with LN-1 (Miner, 1999). Hence it is likely that the β1 and γ1 laminin chains we detect with the polyclonal anti-LN-1 antiserum in fact originate from LN-10. Indeed, when we immunoprecipitated lysates of cyst that were metabolically labeled with [^{35}S]methionine, we pulled down a protein of the predicted size of the α5 laminin chain (~400 kDa) (Ido *et al.*, 2004; (Figure 4G). This suggests that immunoprecipitation with the anti-laminin antiserum pulls down the entire LN-10 heterotrimer, although we cannot rule out the possibility that it is a different laminin. As we found for the $\beta1\gamma1$ chains, AIIB2 treatment neither affected the levels of the α-chain in isolated cyst with associated BM nor the intracellular levels of trypsin-digested cysts (abovementioned pools 3 and 4, respectively).

Together, our data indicate that the altered formation of BM we observe was not due to AIIB2-mediated alterations in synthesis or secretion of laminin per se (Figure 4, E–G).

Exogenous LN-1 Partially Rescues the Normal Cyst Phenotype

When plated in a collagen I matrix supplemented with LN-1, which is capable of self-assembly (Yurchenco and Cheng, 1993), the inverted apical polarity of AIIB2-treated MDCK cells was significantly rescued. Whereas AIIB2-treated cysts had no or only very small lumens (Figure 5A), the addition of LN-1 to these cultures resulted in formation of multiple lumens (Figure 5B). Strikingly, the apical marker (gp135) was now confined to these lumens and largely not found at the periphery of the cysts (Figures 5B). Staining of the tight junction marker occludin confirmed the rescue of normal polarity by exogenous LN-1 in AIIB2 cysts (our unpublished data). This is very similar to the rescue of orientation of polarity that we reported when N17Rac1 cysts were grown in collagen I supplemented with LN-1 (O'Brien *et al.*, 2001). AIIB2 treatment also resulted in perturbation of collagen IV deposition (Figure 4, D and D′), but addition of exogenous collagen IV did not rescue the phenotype (Figure 5C). This finding is consistent with the notion that integration of collagen IV into the BM is a secondary event and depends on initial laminin deposition (Li *et al.*, 2003).

The rescue of the inverted apical polarity by exogenous LN-1 increased over time. In 5-d old cultures, the presence of LN-1 increased the number of AIIB2-treated cysts with an interior apical pole only slightly (25% in a LN-1-containing matrix vs. 20% without LN-1). In 9-d-old cultures, however, LN-1 addition resulted in cultures in which 80% of the cyst had interior apical polarity versus 20% in the 9-d-old control cultures without LN-1 (Figure 5D). We tested whether the time-dependent rescue was due to turnover of AIIB2. When we grew cysts in the presence of AIIB2 in only the medium, and refed cysts every other day with new AIIB2-containing medium, we found no difference, either in the observed phenotype or in the extent to which exogenous LN-1 was able to rescue the phenotype, compared with cysts grown according to our original protocol (our unpublished data). Furthermore, when grown in the presence of 80 μg/ml AIIB2, instead of 8 μg/ml, the extent and time course of phenotypic rescue by exogenous LN-1 was unchanged (our unpublished data). These results show that increased rescue over time was not due to instability of the AIIB2 under these experimental conditions but is consistent with laminin-dependent assembly of BM being a key aspect of polarization.

Activated Rac1 Rescues BM Organization and Cyst Polarity

Our findings that Rac1 is required for β1-integrin-mediated tubulocyst formation (Figure 2) and our previous work that demonstrated a role for Rac1 in laminin organization into BM and polarity development (O'Brien *et al.*, 2001) indicate that a β1 integrin to Rac1 signaling pathway regulates the formation of BM and the subsequent orientation of polarity. To further validate this hypothesis, we tested whether activated V12Rac1 could rescue the inverted polarity in AIIB2-treated cysts. As shown in Figure 2, A and B-10, the expression levels of V12Rac1 in cells grown without Dox were sufficient to completely rescue the AIIB2-induced block on tubulocyst formation upon collagen overlay. However, when we grew cysts from V12Rac1-expressing cells, V12Rac1 expression had diminished below background level in a 7-d-old culture. A similar loss of expression from the tetracycline repressible system during cyst culture has been observed with several other, but not all, of a variety of transfected genes in MDCK cells (our unpublished data). Therefore, before plating cells into collagen, we stimulated

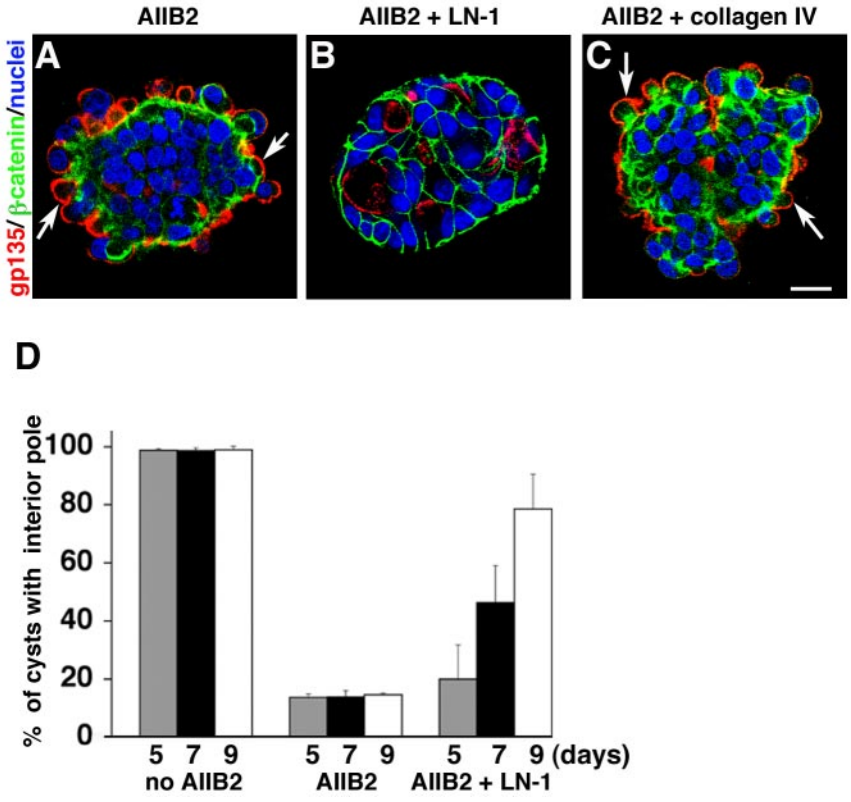

Figure 5. Exogenous LN-1 rescues the normal cyst phenotype. (A–C) Cysts grown in the presence of AIIB2 have inverted polarity (A). Addition of exogenous LN-1 (B) but not collagen IV (C) in AIIB2-treated cysts reverts the apical pole to the luminal surface and induces the formation of lumens. Confocal images represent 7-d-old AIIB2-treated cysts stained with the apical protein marker gp135 (red), basolateral protein, β-catenin (green), and nuclei (blue) in the presence of LN-1 or collagen IV. Arrows in A and C indicate the presence of the apical gp135 at the periphery of the cysts. (D) Quantitation of cyst phenotypes in untreated cysts, AIIB2-treated cysts, and AIIB2-treated cysts with exogenous LN-1 shows that in the presence of exogenous LN-1, the proportion of cysts with an interior pole gradually increases over time. Bar, 10 μm (A–C).

V12Rac1 expression by treating cells grown in a monolayer overnight with 2.5 mM sodium butyrate in the absence of Dox (Jou *et al*., 1998). Six hours after removing the sodium butyrate, cells were trypsinized and suspended in collagen in the absence of Dox. As usual cysts were then grown for 7 d. This overnight treatment with butyrate before plating in collagen yielded expression levels in 7-d-old cysts that were comparable with the expression levels we obtained in the overlay assays (Figure 6A). Furthermore, whereas GTP-Rac1 levels were below detection levels in noninduced cysts (+Dox), high levels of GTP-Rac1 were found in the cysts expressing the V12Rac1 mutant (Figure 6A). Control experiments showed that in untransfected MDCK cells, the brief sodium butyrate treatment did not interfere with the establishment of polarity in cysts, or inversion of polarity upon AIIB2 treatment (our unpublished data).

When cultured in collagen, laminin staining in MDCK cells expressing V12Rac1 looked like a uniform meshwork around the cyst (Figure 6, B and D) and cysts formed with normal polarity (Figure 6, G and I), both with (−Dox) and without (+Dox) V12Rac1 expression. This was in contrast to controls grown in the presence of Dox (i.e., no expression of V12Rac1) and AIIB2, in which laminin distribution was irregular (Figure 6C) and only 35% of the cysts had normal polarity (Figure 6, F and H). Strikingly, expression of V12Rac1 in AIIB2-treated cysts resulted in a full restoration of the laminin staining pattern (compare noninduced cells in Figure 6C to induced cells in Figure 6E). Moreover, when grown in the presence of AIIB2, V12Rac1 expression largely rescued the AIIB2-induced inverted polarity and resulted in cultures in which 80% of the cysts had lumens and an interior apical pole and a correctly oriented basolateral surface, although some cells were often inside the lumen (Figure 6, F and J). This provides additional evidence for a signaling pathway in which β1 integrin-mediated Rac1 activation regulates laminin-initiated assembly of BM, which in turn orients polarity during epithelial morphogenesis.

DISCUSSION

We have used 3D culture systems to analyze how β1 integrins regulate orientation of epithelial cell polarity. Our data are consistent with a model in which collagen I, β1 integrin, Rac1 activation and laminin-dependent organization of BM lie in a reciprocal autocrine pathway that orients MDCK cell polarity in culture. Collagen I activates Rac1 via β1 integrin, at least in the overlay system where this can be most directly assessed. Inhibition of β1 integrin or Rac1 prevents tubulocyst formation in the collagen overlay system and inverses polarity in cysts grown in 3D collagen gels. Activated Rac1 can bypass the β1 integrin block and rescues tubulocyst formation and polarity in the overlay and cyst systems, respectively.

Inhibition of β1 integrin (Figure 4) or Rac1 (O'Brien *et al*., 2001) prevents organization of laminin into a regular BM around the cyst periphery and thereby causes an inversion of polarity. Although the synthesis and secretion of laminin is normal, the overall organization or assembly of laminin into a BM is grossly abnormal with β1 integrin inhibition, as seen at the light microscope level. Ligation of β1 integrins can potentially activate many different signaling pathways that regulate epithelial polarity. Surprisingly, our results show that when β1 integrin function is inhibited, activated Rac1 is sufficient to rescue BM organization, at least at the level of the laminin and collagen IV networks and, to a large extent, can rescue normal orientation of polarity and lumen formation. Finally, exogenous LN-1 included at a sufficiently high concentration to self-assemble (Yurchenco and Cheng, 1993) can overcome both the β1 integrin (Figure 4) and the

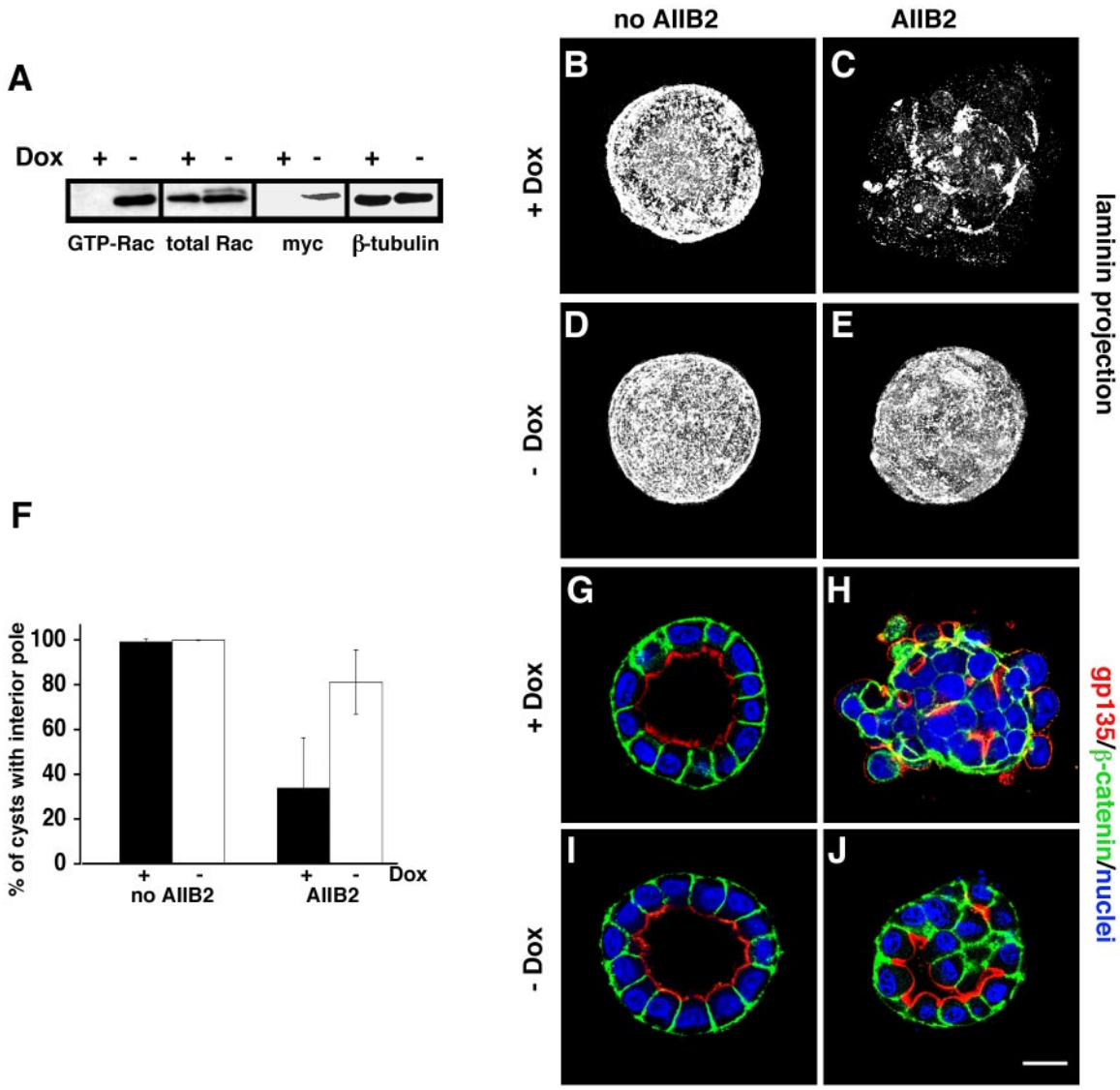

Figure 6. Expression of constitutively active Rac1 induces the establishment of an interior apical pole in the presence of AIIB2. (A) Expression of endogenous and exogenous Rac1 and GTP-Rac1 in MDCK cysts that express V12Rac1 under control of a tetracycline-repressible transactivator. Cysts, grown in the presence or absence of Dox, were cultured for 7 d and Rac activation was analyzed as described in *Materials and Methods*. Levels of endogenous Rac1 and the myc-tagged V12Rac1 mutant were detected by anti-Rac1 and anti-myc antibody. β-Tubulin staining was used as loading control. Note that Rac-GTP levels are below background in noninduced controls (+Dox) and high in V12Rac1-expressing cysts (−Dox). (B–E) Projection of multiple confocal images of V12Rac1-expressing cysts stained for laminin. Noninduced V12Rac1 cells have uniform laminin deposition in untreated cysts (B) and irregular laminin deposition when grown in the presence of AIIB2 (C). V12Rac1 expressing cysts have uniform laminin distribution, in both untreated (D) and AIIB2-treated (E) cultures. (F) Quantitation of V12Rac1 cyst phenotypes, as described in *Materials and Methods*, indicates that 99% of either noninduced or V12Rac1-expressing cysts have normal polarity. In the presence of AIIB2, only 30% of noninduced cysts have normal polarity, whereas expression of V12Rac1 rescues the normal polarity and increases the percentage of cysts with an interior apical pole to 85% of the total population. The graphs represent the means ± SD of three separate experiments. In each experiment, 200 cysts per condition were analyzed. (G–J) Representative confocal images for F. Staining for gp135 (red), β-catenin (green), and nuclei (blue) shows that V12Rac1 cells form cysts with normal polarity (G) and cysts treated with AIIB2 have a peripheral apical pole (H) as described in Figure 3. V12Rac1-expressing cells form normal cysts with gp135 at the luminal surface, in the absence of AIIB2 (I). In the presence of AIIB2, V12Rac1-expressing cells still form cysts with an interior apical pole (J), although the lumen is not as well established as in untreated cysts. Bar, 10 μm.

N17Rac1 block (O'Brien *et al.*, 2001) and can rescue orientation of polarity.

Together, our data and those of many others not only identify several components of a pathway involved in orientation of polarity but also can be interpreted as ordering these components into a simple linear pathway: collagen I → β1 integrin → → Rac1 activation → → laminin organization into nascent BM → → assembly of BM → → orientation of polarity. The entire mechanism is undoubtedly far more complex, both in vitro and especially in vivo. For instance, this model clearly misses many intermediate components. Collagen I likely interacts directly with β1 integrin, but the connections between other components in this model are almost certainly indirect. Nevertheless, by using the simple

model system of MDCK cells in 3D culture, we were able to demonstrate the regulation of the reciprocal relationship between epithelia and the extracellular matrix. Specifically, we show that an initial "outside-in" signaling (β1 integrin to Rac1) is followed by "inside-out" signaling (Rac1 to BM assembly), followed by a second "outside-in" signaling event (BM to orientation of cell polarization). These observations are significant and important because they allow us to understand the relationship of epithelial cells with their matrix in more complex systems.

A role for β1-integrin-mediated signaling in epithelial polarization was initially recognized in kidney development (Sorokin *et al*., 1990). β1 integrin inhibitory antibodies (Klinowska *et al*., 1999) or dominant-negative β1 integrins perturb mammary gland development and cells isolated from these glands do not polarize properly (Faraldo *et al*., 1998). On the other hand, β1 integrin-null keratinocytes localize E-cadherin normally (Brakebusch *et al*., 2000), and β1 integrin inhibitory antibodies restore tissue organization and cell polarity in tumorigenic human breast cells (Weaver *et al*., 1997). The reasons for these apparent opposite results are yet unknown but could result from elevated β1 integrin levels in these tumor cells. Possibly, inhibition of β1 integrins by the antibody restores normal tissue architecture by bringing β1 integrin-mediated signaling to levels similar to nontransformed cells.

We have started to analyze which specific integrin heterodimers and laminin heterotrimers are involved in the signaling pathways mentioned above. Here, we have used a polyclonal antiserum directed against LN-1 (α1β1γ1), a laminin isoform largely absent in adult tissue (Colognato and Yurchenco, 2000). We could not detect α1 laminin by RT-PCR, whereas we detected robust expression of the α3 and α5 laminin chains. Although we cannot exclude the presence of other laminin forms, we believe that the laminin we detect by immunofluorescence, Western blotting, and metabolic labeling most likely represent β1/γ1 chains originating from LN-10 (α5β1γ1), which is the main laminin isoform deposited by kidney epithelia (Miner, 1999).

Consistent with the reported role for β1 integrin in laminin deposition into BM (Faraldo *et al*., 1998; Sasaki *et al*., 1998; Aumailley *et al*., 2000; Lohikangas *et al*., 2001; Li *et al*., 2002), we find that inhibition of β1 integrins with AIIB2 results in marked changes in laminin staining around the cyst periphery. Mammary cells expressing mutant β1 integrins inappropriately deposit laminin at the lateral, instead of the basal surface of cells (Faraldo *et al*., 1998). Possibly, some BM assembles at the interior of the MDCK cysts, which in turn may result in an inverted axis of polarity, perhaps through interaction of laminin with cell surface receptors.

Secretion of the LN-1 heterotrimer can be regulated by synthesis of the α1 (Yurchenco *et al*., 1997) and possibly the α5 chain (Miner and Yurchenco, 2004), and β1-integrin-deficient mouse embryoid bodies are unable to deposit LN-1 or to cavitate due to an inhibition of synthesis of this chain (Aumailley *et al*., 2000; Li *et al*., 2002). Here, we find that synthesis and secretion of the β1 and γ1 laminin chains are unaffected when β1 integrin function is blocked by inhibitory antibodies. In addition, we find that neither the transcription of the α3 and α5 laminin chains nor the secretion of intact laminin β1/γ1-containing heterotrimers (presumably LN-10) is inhibited. Therefore, our data indicate that in MDCK cysts, β1 integrins regulate the organization of BM through an alternative mechanism (see below).

It is unclear why β1 integrins inhibit laminin α chain synthesis in embryoid bodies (Li *et al*., 2002) but not in MDCK cells. Possibly, the synthesis of the α5 laminin and α1 laminin chains, which colocalize early in development, but diverge at later stages (Miner *et al*., 1998), is regulated differentially in fetal and adult tissue. Alternatively, these differences may be due to the fact that different cell systems and methods to inhibit β1 integrins were used. Nevertheless, even though BM assembly in MDCK cyst and embryoid bodies seems mediated through different mechanisms, both the study of Li *et al*. (2002) and the data presented here are consistent with a model in which epithelial morphogenesis is regulated by a β1 integrin-mediated organization of laminin into BM.

Because β1 integrins did not affect the synthesis or secretion of laminin chains, we propose that the altered BM organization in MDCK cysts is mediated further downstream, at the level of laminin-interacting receptors. BM components such as collagen IV and certain laminins (LN1–4, LN-10, and LN-11) are able to self-assemble in vitro (Yurchenco *et al*., 1992; Yurchenco and Cheng, 1993; Miner and Yurchenco, 2004). In vivo, however, cell surface receptors are thought to mediate preferential polymerization of laminin at cell surfaces by increasing its local concentration (Colognato *et al*., 1999; Yurchenco *et al*., 2004). This is likely followed by association of collagen IV polymers, which may stabilize the nascent BM and allow for the incorporation of additional BM components. The receptor that regulates BM assembly at the cell surface has not been unequivocally identified, and multiple different receptors may play redundant roles (Yurchenco *et al*., 2004). Substantial evidence, however, points to a role of α-dystroglycan and β1 integrin-containing integrins in this process (DiPersio *et al*., 1997; Henry and Campbell, 1998; Colognato *et al*., 1999).

α2β1 and α3β1 integrins are the β1 integrin-containing integrins in MDCK cells (Schoenenberger *et al*., 1994). Although both integrins have a broad ligand specificity, the preferred binding partner for LN-10 of these two is α3β1 integrin (Kikkawa *et al*., 1998; Ido *et al*., 2004). Interestingly, α3 integrin levels were reduced by 70–80%, in dominant-negative Rac1-expressing (O'Brien *et al*., 2001) and AIIB2-treated cells, which may point to a role of α3β1 in BM assembly. Note, however, that α2β1, not α3β1 has been shown to be the relevant receptor for collagen I-induced tubulocyst formation (Schwimmer and Ojakian, 1995; Zuk and Matlin, 1996). Alternatively, MDCK cells may bind laminin through α-dystroglycan (Kachinsky *et al*., 1999) or Forssman glycolipid (Zinkl *et al*., 1996). Moreover, the Lutheran glycoprotein, which specifically binds laminin α5 and concentrates at the cell periphery through interaction with LN-10/11 (Moulson *et al*., 2001), may be involved in signaling that regulates the formation of BM. Although expressed in many epithelia, including the kidney (Moulson *et al*., 2001), it is unclear whether MDCK cells endogenously express Lutheran (El Nemer *et al*., 1999).

BM assembly, normal cell polarization and lumen formation in AIIB2-treated cysts can be rescued by an excess of LN-1, as was reported previously for embryoid bodies (Li *et al*., 2002) or by activated Rac1. This suggests that AIIB2 antibodies do not perturb BM assembly by simply masking the binding sites to β1 integrin, consistent with the finding that the AIIB2 and ligand binding sites of β1 integrin do not overlap (Takada and Puzon, 1993). Rather, our data indicate that initial "outside-in" signaling from collagen I to β1 integrin is followed by Rac1-dependent "inside-out" signaling to laminin receptors that facilitate the assembly of BM at the cell surface. Possibly, Rac1 exerts this function by regulating actin through α-dystroglycan and a syntrophin/utrophin complex (Kachinsky *et al*., 1999), because preferential lami-

nin polymerization at cell surfaces depends on the actin cytoskeleton (Colognato *et al*., 1999).

Finally, our data suggest that the laminin-dependent assembly of BM induces a second "outside-in" type signaling, which orients apico-basolateral polarity. This signaling pathway is at least in part independent of Rac1, because the phenotype of N17Rac1-expressing cysts can be partially rescued by exogenous LN-1 (O'Brien *et al*., 2001), which does not activate Rac1 in AIIB2-treated overlay cultures (our unpublished data). This signaling pathway works to orient the cell with the apical surface opposite to the basal surface, where the BM is located. It is yet unclear why we observe that cell polarity is inverted and not scrambled. As mentioned in the Introduction, three major complexes are responsible for polarization, of which the Par3/Par6/aPKC complex is thought to be upstream of the other two. It is tempting to speculate that signaling downstream of assembled BM eventually impacts the Par3/Par6/aPKC complex to determine its location at the apical pole and thus the orientation of the cell.

Although these data can be interpreted in terms of a linear pathway, epithelial morphogenesis is clearly much more complex, especially in vivo. Signaling and morphogenetic pathways are generally part of complex networks with numerous other inputs, as well as many cross-connections and feedback loops at different levels. Nevertheless, this work illustrates the power of simple cell culture systems to begin to understand the cellular basis of complex morphogenetic events, such as assembly of epithelial tissues.

ACKNOWLEDGMENTS

We thank Sandra Huling and the University of California San Francisco Liver Center Core Facility for electron micrographs and the outstanding technical assistance of Gina Whitmore and Holly Weachter. W. Y. is supported by fellowships from the American Heart Association, Western Affiliate (0325013Y and 0120084Y) and from the National Kidney Foundation. A. D. is supported by a fellowship of the Susan G. Komen Breast Cancer Foundation (PDF0100766). P. L. is supported by the French National Center for Scientific Research (Centre National de la Recherche Scientifique). K.S.M was supported by National Institutes of Health R01 DK046768. G. M. was supported by a Shriners Hospital for Children Research Fellowship, an Ethicon Surgical Research Fellowship from the Society of University Surgeons, and National Institutes of Health T32 DK64581. T.-S.J. was supported by a research grant from the National Taiwan University Hospital (NTUH 92-S014). K.E.M is supported by grants of the National Institutes of Health. M. Z. was supported by a fellowship of the American Cancer Society, California Division (2-7-99) and start-up funds from the Department of Surgery, University of Cincinnati.

REFERENCES

Aumailley, M., Pesch, M., Tunggal, L., Gaill, F., and Fassler, R. (2000). Altered synthesis of laminin 1 and absence of basement membrane component deposition in (beta)1 integrin-deficient embryoid bodies. J. Cell Sci. *113*, 259–268.

Brakebusch, C., *et al*. (2000). Skin and hair follicle integrity is crucially dependent on beta 1 integrin expression on keratinocytes. EMBO J. *19*, 3990–4003.

Caplan, M. J., Stow, J. L., Newman, A. P., Madri, J., Anderson, H. C., Farquhar, M. G., Palade, G. E., and Jamieson, J. D. (1987). Dependence on pH of polarized sorting of secreted proteins. Nature *329*, 632–635.

Colognato, H., Winkelmann, D. A., and Yurchenco, P. D. (1999). Laminin polymerization induces a receptor-cytoskeleton network. J. Cell Biol. *145*, 619–631.

Colognato, H., and Yurchenco, P. D. (2000). Form and function: the laminin family of heterotrimers. Dev. Dyn. *218*, 213–234.

DiPersio, C. M., Hodivala-Dilke, K. M., Jaenisch, R., Kreidberg, J. A., and Hynes, R. O. (1997). alpha3beta1 Integrin is required for normal development of the epidermal basement membrane. J. Cell Biol. *137*, 729–742.

El Nemer, W., Colin, Y., Bauvy, C., Codogno, P., Fraser, R. H., Cartron, J. P., and Le Van Kim, C. L. (1999). Isoforms of the Lutheran/basal cell adhesion molecule glycoprotein are differentially delivered in polarized epithelial cells. Mapping of the basolateral sorting signal to a cytoplasmic di-leucine motif. J. Biol. Chem. *274*, 31903–31908.

Etienne-Manneville, S., and Hall, A. (2002). Rho GTPases in cell biology. Nature *420*, 629–635.

Faraldo, M. M., Deugnier, M. A., Lukashev, M., Thiery, J. P., and Glukhova, M. A. (1998). Perturbation of beta1-integrin function alters the development of murine mammary gland. EMBO J. *17*, 2139–2147.

Giancotti, F. G., and Ruoslahti, E. (1999). Integrin signaling. Science *285*, 1028–1032.

Hall, A. (1998). Rho GTPases and the actin cytoskeleton. Science *279*, 509–514.

Hansen, S., Zegers, M., Woodrow, M., Rodriguez-Viciana, P., Chardin, P., Mostov, K., and McMahon, M. (2001). Induced expression of Rnd3 is associated with transformation of polarized epithelial cells by the Raf-MEK-extracellular signal-regulated kinase pathway. Mol. Cell. Biol. *20*, 9364–9375.

Henry, M. D., and Campbell, K. P. (1998). A role for dystroglycan in basement membrane assembly. Cell *95*, 859–870.

Ido, H., *et al*. (2004). Molecular dissection of the alpha-dystroglycan- and integrin-binding sites within the globular domain of human laminin-10. J. Biol. Chem. *279*, 10946–10954.

Jou, T.-S., and Nelson, W. (1998). Effects of regulated expression of mutant RhoA and Rac1 small GTPases on the development of epithelial (MDCK) cell polarity. J. Cell Biol. *147*, 85–100.

Jou, T.-S., Schneeberger, E., and Nelson, W. (1998). Structural and functional regulation of tight junctions by RhoA and Rac1 small GTPases. J. Cell Biol. *142*, 101–115.

Kachinsky, A. M., Froehner, S. C., and Milgram, S. L. (1999). A PDZ-containing scaffold related to the dystrophin complex at the basolateral membrane of epithelial cells. J. Cell Biol. *145*, 391–402.

Kikkawa, Y., Sanzen, N., and Sekiguchi, K. (1998). Isolation and characterization of laminin-10/11 secreted by human lung carcinoma cells. laminin-10/11 mediates cell adhesion through integrin alpha3 beta1. J. Biol. Chem. *273*, 15854–15859.

Klinowska, T. C., Soriano, J. V., Edwards, G. M., Oliver, J. M., Valentijn, A. J., Montesano, R., and Streuli, C. H. (1999). Laminin and beta1 integrins are crucial for normal mammary gland development in the mouse. Dev. Biol. *215*, 13–32.

Leroy, P., Berto, F., Bourget, I., and Rossi, B. (2004). Down-regulation of Hox A7 is required for cell adhesion and migration on fibronectin during early HL-60 monocytic differentiation. J. Leukoc. Biol. *75*, 680–688.

Li, S., Edgar, D., Fassler, R., Wadsworth, W., and Yurchenco, P. D. (2003). The role of laminin in embryonic cell polarization and tissue organization. Dev. Cell *4*, 613–624.

Li, S., Harrison, D., Carbonetto, S., Fassler, R., Smyth, N., Edgar, D., and Yurchenco, P. D. (2002). Matrix assembly, regulation, and survival functions of laminin and its receptors in embryonic stem cell differentiation. J. Cell Biol. *157*, 1279–1290.

Lohikangas, L., Gullberg, D., and Johansson, S. (2001). Assembly of laminin polymers is dependent on beta1-integrins. Exp. Cell Res. *265*, 135–144.

Macara, I. G. (2004). Parsing the polarity code. Nat. Rev. Mol. Cell. Biol. *5*, 220–231.

Meadus, W. J. (2003). A semi-quantitative RT-PCR method to measure the in vivo effect of dietary conjugated linoleic acid on porcine muscle PPAR gene expression. Biol. Proced. Online *5*, 20–28.

Miner, J. H. (1999). Renal basement membrane components. Kidney Int. *56*, 2016–2024.

Miner, J. H., Cunningham, J., and Sanes, J. R. (1998). Roles for laminin in embryogenesis: exencephaly, syndactyly, and placentopathy in mice lacking the laminin alpha5 chain. J. Cell Biol. *143*, 1713–1723.

Miner, J. H., and Yurchenco, P. D. (2004). Laminin Functions in Tissue Morphogenesis. Annu. Rev. Cell Dev. Biol. *20*, 255–284.

Mostov, K., Su, T., and ter Beest, M. (2003). Polarized epithelial membrane traffic: conservation and plasticity. Nat. Cell Biol. *5*, 287–293.

Moulson, C. L., Li, C., and Miner, J. H. (2001). Localization of Lutheran, a novel laminin receptor, in normal, knockout, and transgenic mice suggests an interaction with laminin alpha5 in vivo. Dev. Dyn. *222*, 101–114.

Nelson, W. J. (2003). Adaptation of core mechanisms to generate cell polarity. Nature *422*, 766–774.

O'Brien, L. E., Jou, T. S., Pollack, A. L., Zhang, Q., Hansen, S. H., Yurchenco, P., and Mostov, K. E. (2001). Rac1 orientates epithelial apical polarity through effects on basolateral laminin assembly. Nat. Cell Biol. *3*, 831–838.

O'Brien, L. E., Zegers, M. M., and Mostov, K. E. (2002). Opinion: building epithelial architecture: insights from three-dimensional culture models. Nat. Rev. Mol. Cell. Biol. *3*, 531–537.

Ojakian, G. K., Ratcliffe, D. R., and Schwimmer, R. (2001). Integrin regulation of cell-cell adhesion during epithelial tubule formation. J. Cell Sci. *114*, 941–952.

Ojakian, G. K., and Schwimmer, R. (1994). Regulation of epithelial cell surface polarity reversal by beta 1 integrins. J. Cell Sci. *107*, 561–576.

Pollack, A. L., Runyan, R. B., and Mostov, K. E. (1998). Morphogenetic mechanisms of epithelial tubulogenesis: MDCK cell polarity is transiently rearranged without loss of cell-cell contact during scatter factor/hepatocyte growth factor-induced tubulogenesis. Dev. Biol. *204*, 64–79.

Price, L., Leng, J., Schwartz, M., and Bokoch, G. (1998). Activation of rac and cdc42 by integrins mediates cell spreading. Mol. Biol. Cell *9*, 1863–1871.

Roh, M. H., and Margolis, B. (2003). Composition and function of PDZ protein complexes during cell polarization. Am. J. Physiol. *285*, F377–F387.

Sasaki, T., Forsberg, E., Bloch, W., Addicks, K., Fassler, R., and Timpl, R. (1998). Deficiency of beta 1 integrins in teratoma interferes with basement membrane assembly and laminin-1 expression. Exp. Cell Res. *238*, 70–81.

Schoenenberger, C. A., Zuk, A., Zinkl, G. M., Kendall, D., and Matlin, K. S. (1994). Integrin expression and localization in normal MDCK cells and transformed MDCK cells lacking apical polarity. J. Cell Sci. *107*, 527–541.

Schwimmer, R., and Ojakian, G. (1995). The alpha 2 beta 1 integrin regulates collagen-mediated MDCK epithelial membrane remodeling and tubule formation. J. Cell Sci. *108*, 2487–2498.

Sorokin, L., Sonnenberg, A., Aumailley, M., Timpl, R., and Ekblom, P. (1990). Recognition of the laminin E8 cell-binding site by an integrin possessing the alpha 6 subunit is essential for epithelial polarization in developing kidney tubules. J. Cell Biol. *111*, 1265–1273.

Takada, Y., and Puzon, W. (1993). Identification of a regulatory region of integrin beta 1 subunit using activating and inhibiting antibodies. J. Biol. Chem. *268*, 17597–17601.

Van Aelst, L., and Symons, M. (2002). Role of Rho family GTPases in epithelial morphogenesis. Genes Dev. *16*, 1032–1054.

Vega-Salas, D. E., Salas, P. J., Gundersen, D., and Rodriguez-Boulan, E. (1987). Formation of the apical pole of epithelial (Madin-Darby canine kidney) cells: polarity of an apical protein is independent of tight junctions while segregation of a basolateral marker requires cell-cell interactions. J. Cell Biol. *104*, 905–916.

Wang, A. Z., Ojakian, G. K., and Nelson, W. J. (1990a). Steps in the morphogenesis of a polarized epithelium. I. Uncoupling the roles of cell-cell and cell-substratum contact in establishing plasma membrane polarity in multicellular epithelial (MDCK) cysts. J. Cell Sci. *95*, 137–151.

Wang, A. Z., Ojakian, G. K., and Nelson, W. J. (1990b). Steps in the morphogenesis of a polarized epithelium. II. Disassembly and assembly of plasma membrane domains during reversal of epithelial cell polarity in multicellular epithelial (MDCK) cysts. J. Cell Sci. 153–165.

Weaver, V., Petersen, O., Wang, F., Larabell, C., Briand, P., Damsky, C., and Bissell, M. (1997). Reversion of the malignant phenotype of human breast cells in three-dimensional culture and in vivo by integrin blocking antibodies. J. Cell Biol. *137*, 231–245.

Yeaman, C., Grindstaff, K. K., and Nelson, W. J. (1999). New perspectives on mechanisms involved in generating epithelial cell polarity. Physiol. Rev. *79*, 73–98.

Yu, W., O'Brien, L. E., Wang, F., Bourne, H., Mostov, K. E., and Zegers, M. M. (2003). Hepatocyte growth factor switches orientation of polarity and mode of movement during morphogenesis of multicellular epithelial structures. Mol. Biol. Cell *14*, 748–763.

Yurchenco, P. D., Amenta, P. S., and Patton, B. L. (2004). Basement membrane assembly, stability and activities observed through a developmental lens. Matrix Biol. *22*, 521–538.

Yurchenco, P. D., and Cheng, Y. S. (1993). Self-assembly and calcium-binding sites in laminin. A three-arm interaction model. J. Biol. Chem. *268*, 17286–17299.

Yurchenco, P. D., Cheng, Y. S., and Colognato, H. (1992). Laminin forms an independent network in basement membranes. J. Cell Biol. *117*, 1119–1133.

Yurchenco, P. D., Quan, Y., Colognato, H., Mathus, T., Harrison, D., Yamada, Y., and O'Rear, J. J. (1997). The alpha chain of laminin-1 is independently secreted and drives secretion of its beta- and gamma-chain partners. Proc. Natl. Acad. Sci. USA *94*, 10189–10194.

Zahir, N., Lakins, J. N., Russell, A., Ming, W., Chatterjee, C., Rozenberg, G. I., Marinkovich, M. P., and Weaver, V. M. (2003). Autocrine laminin-5 ligates alpha6beta4 integrin and activates RAC and NFkappaB to mediate anchorage-independent survival of mammary tumors. J. Cell Biol. *163*, 1397–1407.

Zegers, M. M., O'Brien, L. E., Yu, W., Datta, A., and Mostov, K. E. (2003). Epithelial polarity and tubulogenesis in vitro. Trends Cell Biol. *13*, 169–176.

Zinkl, G. M., Zuk, A., van der Bijl, P., van Meer, G., and Matlin, K. S. (1996). An antiglycolipid antibody inhibits Madin-Darby canine kidney cell adhesion to laminin and interferes with basolateral polarization and tight junction formation. J. Cell Biol. *133*, 695–708.

Zuk, A., and Matlin, K. S. (1996). Apical beta 1 integrin in polarized MDCK cells mediates tubulocyst formation in response to type I collagen overlay. J. Cell Sci. *109*, 1875–1889.